Seasonal Variation of Liquid and Ice Water Path in Nonprecipitating Clouds over Oceans

BING LIN

College of William and Mary, Williamsburg, Virginia

WILLIAM B. ROSSOW

NASA/Goddard Institute for Space Studies, New York, New York

(Manuscript received 14 June 1995, in final form 30 April 1996)

ABSTRACT

Seasonal variations of liquid and ice water paths (LWP and IWP) in nonprecipitating clouds over oceans are estimated for 4 months by combining the International Satellite Cloud Climatology Project (ISCCP) and Special Sensor Microwave/Imager (SSM/I) data. The ISCCP data are used to separate clear/cloudy skies and warm/cold clouds and to determine cloud optical thickness, cloud-top temperature, and sea surface temperature. SSM/I data are used to separate precipitating and nonprecipitating clouds and to determine LWP. About 93% of all clouds are nonprecipitating clouds, and about half of nonprecipitating clouds are warm (cloud-top temperature > 0°C). The average LWP for warm nonprecipitating clouds is about 6 mg cm^{-2}. The values of total water path obtained from the ISCCP values of optical thickness for cold nonprecipitating clouds are larger than the LWP values from SSM/I, which the authors explain in terms of IWP. The average IWP for cold nonprecipitating clouds is about 7 mg cm^{-2}, with LWP being about 5 mg cm^{-2}. Tropical and cold hemisphere clouds have higher IWP values (around 10 mg cm^{-2}) than those in warm hemispheres; whereas LWP values for warm nonprecipitating clouds vary little with latitude or season. Ice fractions, IWP/(LWP + IWP), in cold nonprecipitating clouds increase systematically with decreasing cloud-top temperatures, reaching 50% at about -15°C but ranging from about -5° to -10°C in the northern midlatitudes in autumn and the Tropics year-round to about -25°C in the southern midlatitudes in summer. The ratio of IWP to LWP in *cold* nonprecipitating clouds reaches almost 3 in the northern midlatitudes in autumn and falls as low as 0.6 in the southern midlatitudes in spring–summer. Combining warm and cold nonprecipitating clouds gives a global ratio of IWP to LWP that is about 0.7 over oceans.

1. Introduction

Differences in modeling the transition between liquid and ice phases in clouds produce large variations in GCM cloud–climate feedback, even changing it from positive to negative (Li and Le Treut 1992). Mitchell et al. (1989) found that their climate model sensitivity to a doubling of CO_2 was much smaller when using Smith's (1990) cloud prediction scheme than when using a relative humidity scheme. A substantial part of the difference was due to different magnitude reductions of the probability of ice phase clouds in the warmer model climate. These results suggest that the correct partitioning of cloud water between liquid and ice phases is a crucial feature of producing realistic cloud distributions in GCMs that determine the fidelity of their simulations of the earth's radiation budget and climate (Smith 1990).

Cloud formation and decay processes are most naturally formulated in terms of the liquid and ice water contents (LWC and IWC), the average particle radius (r), and the vertical extent, whereas interactions of clouds and radiation (including remote sensing of clouds) are formulated in terms of optical thickness (τ) and effective particle radius (r_e), as well as particle shape, single scattering albedo, and asymmetry parameter. Both sets of variables can be linked to the column liquid and ice water paths (LWP and IWP). Unfortunately, quantitative knowledge of these cloud properties and the processes that influence them remain incomplete (Del Genio 1993; Del Genio et al. 1996).

Observations of the transition between water and ice in clouds are very infrequent due to the expense and difficulty of in situ experiments, but there are many case studies (Sassen and Zhao 1993; Sassen 1991; Gamache 1990; Platt et al. 1987; Hobbs and Rangno 1985 and references therein). These studies show that liquid water is frequently observed in clouds at temperatures below its thermodynamic freezing temperature (0°C). Hobbs and Rangno (1985) suggest that cloud water more commonly starts to freeze at about -4°C over oceans and about -10°C over land. Sassen et al. (1989) and Feigelson (1984) report occurrences of supercooled droplets at temperatures as cold as -40°C. The

Corresponding author address: Dr. Bing Lin, MS 420, NASA Langley Research Center, Hampton, VA 23681-0001.

variability in freezing temperatures among these observations probably reflects a dependence of the transition of water to ice on factors such as the age of the particles, cloud condensation nuclei (aerosol) characteristics, meteorological situation (cloud types), and climate regime (latitude and season).

If we assume that the amount of cloud water is proportional to the amount of water condensed from a saturated parcel lifted over small pressure intervals, then the ratio of column ice water (the freezing level is at −4°C to the tropopause) to liquid water (lifting the condensation level to the freezing level) in a global-mean temperature profile is about 0.9 (see appendix). The actual ratio will be influenced by the processes controlling cloud water content and its vertical, horizontal, and seasonal distributions.

No long-term global survey of the relative amounts of liquid and ice water has been conducted because distinguishing the two phases with available satellite remote sensing measurements is also difficult. Available microwave measurements are insensitive to cloud ice because the index of refraction makes ice absorption insignificant and the particles are too small to scatter much radiation. Available infrared measurements can only determine the phase of the uppermost portion of the clouds (Carlson et al. 1993), and available visible measurements are sensitive to cloud particle shapes and sizes. The refractive indexes of ice and water are similar at the visible wavelengths.

Recent advances in the retrieval of cloud properties from satellite measurements include: optical thickness (Rossow et al. 1989; Rossow et al. 1991), LWP (Greenwald et al. 1993; Liu and Curry 1993), and liquid droplet radius (Han et al. 1994). However, global observations of IWP and ice particle sizes do not exist yet. The results of Lin and Rossow (1994) suggested a possible method for inferring IWP. The purpose of this study is to extend the results of Lin and Rossow (1994) to investigate global-scale seasonal variations of LWP and IWP in nonprecipitating clouds. The global (excluding polar regions) datasets and retrieval methods are briefly described in section 2. Section 3 examines the seasonal variations of oceanic cloud cover, total LWP (precipitating and nonprecipitating clouds), column water vapor (CWV), and LWP and IWP for nonprecipitating clouds. Section 4 discusses the sources of uncertainty in these estimates of IWP.

2. Datasets and analysis method

The key to separating LWP and IWP is combining visible, infrared, and microwave radiance measurements (Lin and Rossow 1994). The optical remote sensing method (visible and infrared wavelengths) is much more sensitive to cloud water, including ice, than the analysis of microwaves. The infrared and visible radiances are used to separate cloudy from clear scenes, to classify clouds into two cloud-top temperature categories (cold, $T_c < 0$°C, and warm, $T_c \geq 0$°C), and to obtain cloud optical thickness, from which the total cloud water path (WP, liquid plus ice water path) can be obtained with an assumed particle size. Sea surface temperatures are also retrieved from the infrared radiances. Microwave radiances [brightness temperatures (Tb) with two polarization directions] are used to retrieve both column water vapor and cloud liquid water path. The microwave measurements also indicate whether precipitation is present (Lin and Rossow 1994).

The optical remote sensing data are from the International Satellite Cloud Climatology Project (ISCCP, Rossow and Schiffer 1991). We use the pixel-level results: each pixel is about 5 km in size and sampled at intervals of 30 km and 3 h. The dataset reports for each pixel the following information: satellite name, earth location, surface type (land/water/coast), snow/ice presence, cloud/no-cloud decision, surface reflectivity and temperature, and the cloud optical thickness and cloud-top temperature/pressure (if the pixel is cloudy). In the ISCCP analysis, clear pixels are defined as those with visible (VIS, wavelength ~ 0.6 μm) and infrared (wavelength ~ 11 μm) radiances that do not differ from inferred VIS and IR radiance values for clear conditions by more than predetermined threshold amounts (Rossow and Garder 1993). All other pixels are labeled as cloudy.

The ISCCP analysis retrieves visible optical thicknesses from visible radiances, assuming a uniform plane-parallel cloud layer that is composed of spherical liquid water droplets specified by a gamma distribution with an effective particle radius, $r_e = 10$ μm, and an effective size variance of 0.15 (Rossow et al. 1989, 1991). For the assumed microphysics, the total water path is

$$\mathrm{WP} = \frac{0.6292\tau r_e}{10}, \qquad (1)$$

where r_e is in microns and WP in mg cm^{-2}. The coefficient is exact for the particular size distribution used in the ISCCP retrieval model with $r_e = 10$ μm, but is only approximate for other sizes. Ice particles influence cloud visible reflectivity only a little less efficiently than water droplets, so that ice crystals and ice clouds are also detected in the ISCCP analysis and contribute to the value of total cloud water path. In the current analysis, Eq. (1) is used without regard to the phase of the cloud and r_e is assumed to be 10 μm (see section 4).

The Special Sensor Microwave/Imager (SSM/I) is a passive microwave radiometer that measures brightness temperatures at frequencies of 19.35, 22.235, 37.0, and 85.5 GHz. Both horizontal and vertical polarization measurements are taken at 19.35, 37.0, and 85.5 GHz, while only vertical polarization is measured at 22.235 GHz. The lower three frequencies of SSM/I are used

in this study because the 85-GHz vertical channel is significantly noisier than others, and the brightness temperatures of the lower frequencies are less effectively scattered by cloud and precipitation particles than 85-GHz channels (cf. Wilheit et al. 1991; Lin and Rossow 1994; Lin 1995). For nonprecipitating clouds, microwave radiation depends on the surface emission and the absorption by atmospheric oxygen, water vapor, and cloud liquid water (cf. Petty 1990; Greenwald et al. 1993; Lin and Rossow 1994; Lin 1995). Since ice particles produce very weak absorption and emission at microwave wavelengths, microwave radiances will be completely insensitive to ice particles that are too small (<150 μm) to produce significant scattering (Warren 1984; Wilheit et al. 1977, 1991; Mugnai and Smith 1988; Smith and Mugnai 1988; Adler et al. 1991). The SSM/I analysis follows the method of Greenwald et al. (1993), which is an absorption- and emission-based method that retrieves both LWP and CWV from brightness temperatures at 19 and 37 GHz (Greenwald et al. 1993; Lin and Rossow 1994; Lin 1995). The scheme is modified by using the ISCCP cloud/no-cloud decision, and values of cloud-top temperature (note that we use ISCCP cloud-top temperature as cloud liquid water temperature for warm clouds, while for cold clouds we set cloud liquid water temperature to be 0°C) and surface temperature (Lin and Rossow 1994). Because of uncertainties in the surface properties and the water absorption coefficients, the ISCCP-determined clear scenes are used to adjust the microwave retrieval scheme so that LWP is zero on average in each 2.5° grid box in each month (Lin and Rossow 1994; see also Liu and Curry 1993). The LWP errors in individual retrievals (Lin and Rossow 1994) are larger than those of some studies (Petty 1990; Greenwald et al. 1993). The reason is, we think, that the CWV errors in current microwave retrieval algorithms are larger (Lin and Rossow 1994; also cf. Petty 1990; Greenwald et al. 1993; Tjemkes et al. 1991; Sheu and Liu 1995).

For precipitating clouds, the larger particles, whether liquid or ice, also scatter microwave radiation, so that an emission-based analysis scheme will underestimate the total LWP. Since scattering reduces the difference between the Tb at 37 GHz for vertical and horizontal polarization (Goodberlet et al. 1990; Lin 1995), we use this difference to detect precipitation (if it is >37 K, there is no precipitation). Since scattering by precipitation-sized particles is relatively weak at 19 GHz and 37 GHz (cf. Wilheit et al. 1991; Adler et al. 1990, 1991; Liu and Curry 1992; Lin 1995), our determination of LWP is not sensitive to the precise precipitation cutoff (Liu and Curry 1993; Lin and Rossow 1994). The errors in the LWP due to the cutoff used in this study are less than 10%.

Since the optical remote sensing method is sensitive to both liquid water and ice, while the microwave method is only sensitive to LWP, we use the differences between colocated optically estimated total WP and microwave-estimated LWP to estimate IWP for cold-topped nonprecipitating clouds. Because of the large uncertainties in the colocation, the optical treatment of ice clouds, and the microwave retrievals of LWP, we treat this estimate of IWP as very crude (see discussion in section 4).

In this study, 4 months (August 1987, November 1987, February 1988, and May 1988) in the first annual cycle of SSM/I data are combined with ISCCP at pixel resolution over oceans between 50°S and 50°N. To match ISCCP and SSM/I observations, the time difference between the two observations is required to be ≤ 1.5 h, and the distance between the centers of the ISCCP and SSM/I pixels is required to be ≤ 30 km. In cases of multiple matches, the pixel pair with the minimum separation distance is used (Lin and Rossow 1994). Since we require the ISCCP retrievals of cloud optical thickness, the matchups are restricted to local daytime. This restriction produces low sampling frequencies at higher latitudes in the winter hemisphere. The monthly mean values are aggregated at 2.5° spatial resolution.

3. Seasonal variations of liquid and ice water paths

To frame the discussion of the seasonal variations of LWP and IWP in nonprecipitating clouds, we first compare the global patterns of total cloud cover from ISCCP and total LWP (nonprecipitating and precipitating clouds) and CWV from SSM/I. These statistics are based on both daytime and nighttime retrievals from both datasets. At the beginning of the annual cycle in our analysis (August 1987), the 1986–87 El Niño–Southern Oscillation event was nearing an end (cf. Ropelewski 1988 and references therein): SST patterns are normal during the 4 months analyzed, but the August 1987 cloudiness pattern in the tropical central Pacific is still somewhat anomalous. Thus, the annual cycle represented by these 4 months of data may be slightly distorted from "normal."

Figure 1 compares the monthly zonal-mean distributions of CWV and total LWP from SSM/I in the upper panels, and the total LWP and cloud cover from ISCCP in the lower panels. There is 200–300 times more water in vapor form than in liquid form (note the difference in scales in the figure); adding the estimated ice water amounts may double the total condensed water (see below, cf. Peixoto and Oort 1992). The stronger influence of atmospheric circulation on clouds is indicated by the fact that neither cloud cover nor LWP follows the general latitudinal distribution of CWV. The low-latitude variation of CWV basically follows the decrease of atmospheric temperature, except that the contrast between the tropical maximum (almost 5 g cm^{-2} or 5000 mg cm^{-2}) and subtropical values of CWV is exaggerated by the Hadley circulation (e.g., Tjemkes et al. 1991).

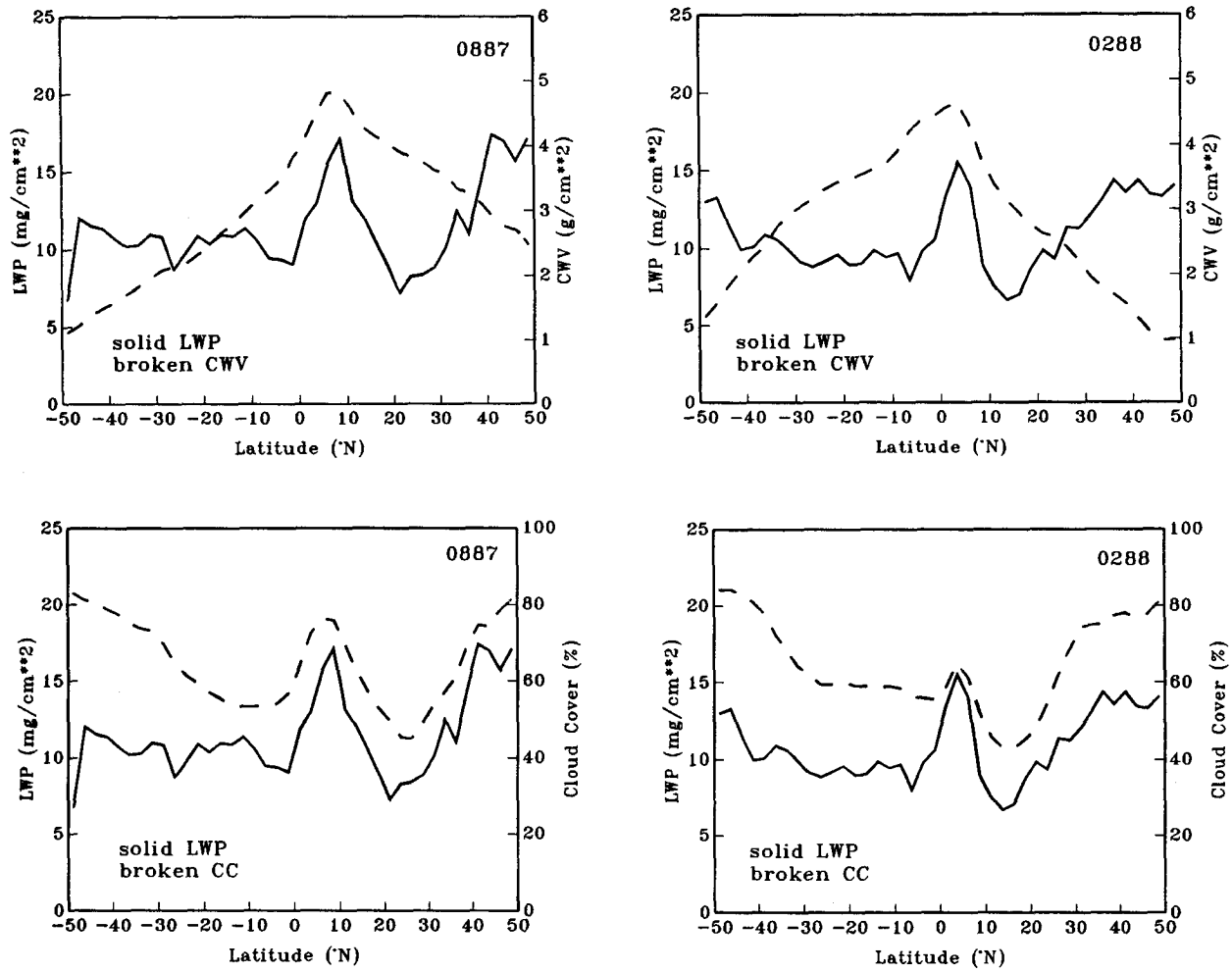

FIG. 1. Monthly zonal-mean distributions of (upper panels) column water vapor (g cm^{-2}; broken curves) and total cloud liquid water path (mg cm^{-2}, precipitating and nonprecipitating, solid curves) from SSM/I for August 1987 (left) and February 1988 (right) and (lower panels) total LWP (solid curves) and ISCCP cloud amounts (percentages; broken curves).

The latitudinal variations of LWP and cloud cover are fairly similar and larger than the variations of CWV, but there are also some notable differences between the cloud cover and LWP distributions. The Hadley circulation is associated with a large concentration of clouds with large LWP (15–17 mg cm^{-2}) near the equator, which shifts latitude with season, and two subtropical zones with smaller amounts of cloud cover and much smaller LWP values (about 7 mg cm^{-2}). The near-equatorial zone of large cloud cover extends over a slightly larger range of latitudes than does the zone of large LWP, consistent with the spreading of cirrus cover away from the more concentrated convective source. This interpretation is reinforced by the fact that almost two-thirds of the total LWP in the Tropics is associated with precipitating clouds, even though such clouds represent less than 10% of the total cloudiness (Table 1). The near-equatorial concentration is farthest north in August 1987 and farthest south in February 1988; the subtropical low concentrations extend poleward most in the summer hemispheres. The subtropical marine stratocumulus regimes exhibit significant seasonal variations in LWP but not as much in total cloud cover. These geographic and seasonal variations show that changes in cloud cover alone are not sufficient to describe cloud radiative effects (Rossow and Lacis 1990; Rossow and Zhang 1995).

The Walker circulation over the Pacific basin is more noticeable in the east–west contrast of LWP and CWV than in the cloud cover (not shown) because the marine stratus regime has large cloud cover but only modest LWP ($\geq$10 mg cm^{-2}), as compared to the peak value of about 20 mg cm^{-2} in the western Pacific.

Secondary maxima in cloud cover and total LWP (13–15 mg cm^{-2}) appear in the midlatitudes in the

TABLE 1. Relative frequencies (as percentages) of cloud types defined by whether cloud-top temperature is above (warm = W) or below (cold = C) 0°C and by whether there is precipitation present (P) or not (NP). Total clouds are indicated by T. These data are listed in four climatological regimes: global (50°S–50°N), Tropics (20°S–20°N), Northern Hemispheric midlatitudes (20°–50°N), and Southern Hemispheric midlatitudes (20°–50°S). Note that Table 2 and Fig. 5 have the same definition for the climatological regimes. Some related values (e.g., W, CP/P, CNP/NP, etc.) can also be calculated from this table.

	Global	Tropics	Northern Hemispheric	Southern Hemispheric
T	65.5	58.0	67.1	73.4
C	33.8	26.9	30.8	41.6
P/T	6.9	8.8	5.4	5.7
WNP/NP	50.1	57.2	56.9	45.3
WP/W	1.9	2.8	1.2	1.3
CP/C	11.6	15.8	10.4	9.1
WP/P	13.3	16.7	11.6	9.6

zone of cyclonic storms, even though CWV values are only about 1–2 g cm^{-2}, less than half the tropical value. The midlatitude values of CWV and LWP are larger in the summer hemisphere than in the winter hemisphere, even though total cloud amounts are about the same in both hemispheres in both seasons. In the midlatitudes only about 5% of total cloudiness is associated with precipitation (Table 1), but these cloud contribute 30%–50% of the total LWP in the midlatitudes. The seasonal variation of LWP is smaller in the Southern Hemisphere than in the Northern Hemisphere, but the annual averaged LWP is larger in the Northern Hemisphere than in the Southern. It may be that the larger temperature contrasts between land and ocean in the Northern Hemisphere that produce greater baroclinic instability also produce thicker clouds than in the Southern Hemisphere. The Northern Hemisphere storm track also exhibits a noticeable equatorward shift from about 40°–50°N to 30°–40°N in winter (February 1988), whereas the Southern Hemisphere storm track appears to remain at about the same location near 45°S year-round (cf. Rossow et al. 1993). Because we truncate the analysis at 50° in each hemisphere, we miss the seasonal variations of LWP at higher latitudes, which are left for future study.

Table 1 summarizes the distribution of cloud types for the 4 months in terms of whether cloud-top temperature is above or below 0°C and whether there is precipitation present or not. Consistent with the first results shown in Lin and Rossow (1994), nearly half of cold and warm clouds are precipitating when LWP reaches about 40 and 50 mg cm^{-2}, respectively; these onset values appear to be slightly larger in the southern midlatitudes than elsewhere and exhibit little seasonal variation. There are no nonprecipitating clouds with LWP > 80 mg cm^{-2}. Globally, only about 6%–7% of all clouds detected by ISCCP exhibit a microwave signature indicating the presence of precipitation; more than 85% of these are cold clouds. Nonprecipitating clouds are near-equally separated into warm and cold types. Hence, the radiation balance of the earth is dominated by the much more common nonprecipitating clouds, whereas latent heat exchanges are dominated by a rare cloud type; these two processes are coupled through the large-scale atmospheric circulation.

a. Warm nonprecipitating clouds

Figure 2 shows the monthly zonal-mean WP values from ISCCP and SSM/I for warm clouds for all 4 months. Since these clouds are composed of relatively small liquid water droplets, the ISCCP values should agree with the SSM/I LWP values if the assumed droplet size (10 μm) in Eq. (1) is about right; the agreement is good (Lin and Rossow 1994; Lin 1995), consistent with independent confirmation that the global-mean droplet size is about 11.5 μm (Han et al. 1994). This comparison forms the basis for using the matched datasets to separate LWP from IWP.

The LWP for warm nonprecipitating clouds is about 6 mg cm^{-2}, with little variation with latitude or season. Comparison with Fig. 1 shows that the relative contribution of LWP from precipitating clouds is larger in the Tropics than in the midlatitudes. Tselioudis et al. (1992) found that the variations of optical thickness of low-level clouds, especially warm clouds, with season and latitude are about 20%. The only significant change in LWP values shown in Fig. 2 occurs in the Northern Hemisphere midlatitudes during August 1987, which is associated with an increase in the frequency of precipitating systems during this period (cf. Lin 1995). Wang and Rossow (1995) report an average cloud-layer thickness for low clouds over oceans < 800 m; hence, an average LWP of 6 mg cm^{-2} is equivalent to a liquid water content of >0.075 g m^{-3}. Eight months of observations of marine stratocumulus clouds from surface instruments off the coast of California exhibit a mean LWP of 7.5 mg cm^{-2} (Fairall et al. 1990). In situ measurements of LWC during the First ISCCP Regional Experiment in July 1987 indicate LWC values of 0.3–0.6 g m^{-3}; but since the cloud-layer thicknesses are only 200–300 m (Blaskovic et al. 1991), these clouds have LWP values of 6–18 mg cm^{-2}. Our average value of LWP is equivalent to an LWC of 0.2 g m^{-3} if average layer thicknesses are 300 m.

b. Cold nonprecipitating clouds

Cold nonprecipitating clouds are more complicated than warm nonprecipitating clouds because of different variations of LWP and IWP. Figure 3 shows the monthly zonal-mean values of WP from ISCCP and LWP from SSM/I for these clouds. The latitude variations of the SSM/I LWP values for the 4 months are similar, increasing from tropical low values around 2–3 mg cm^{-2} to almost 10 mg cm^{-2} in midlatitude storm

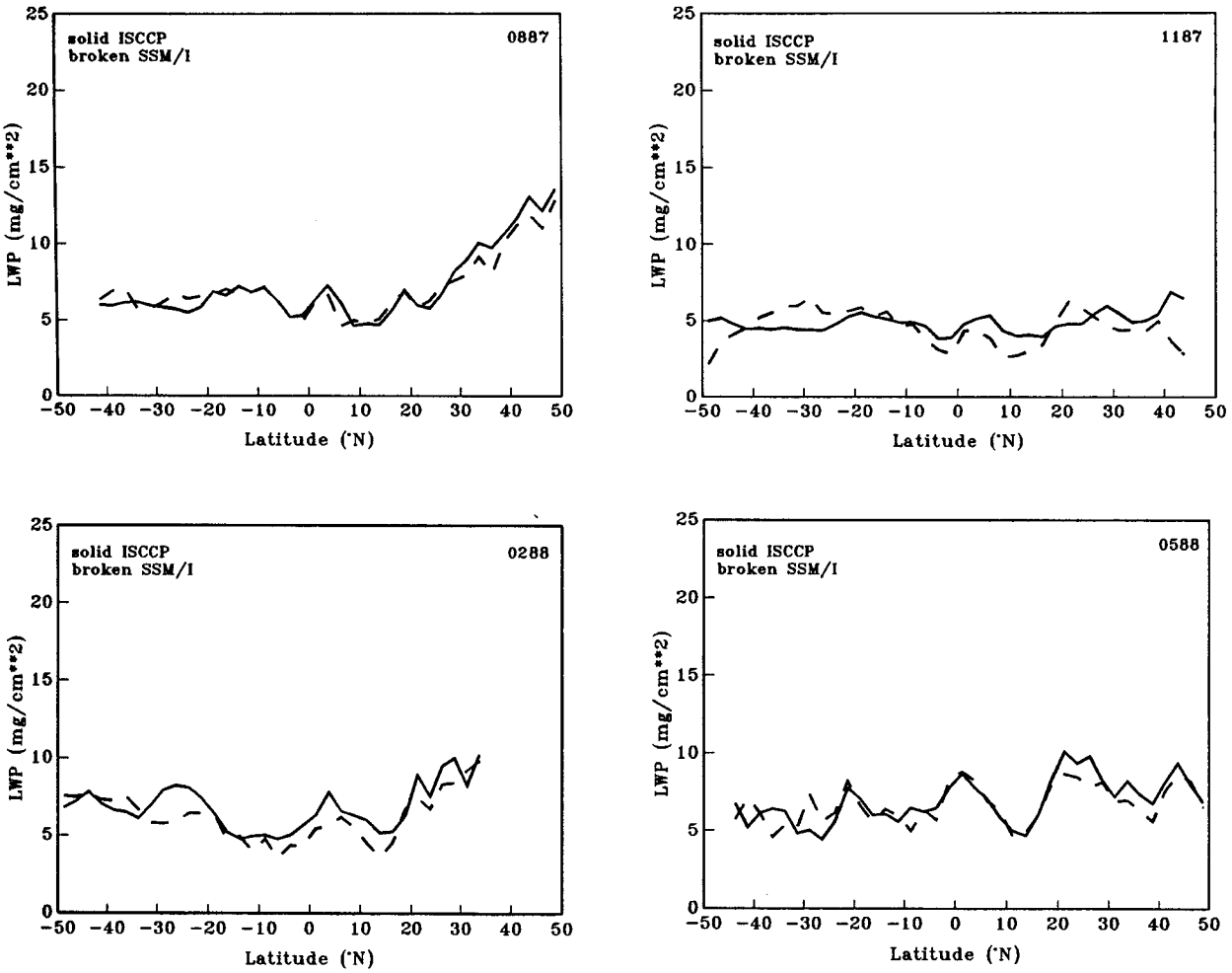

FIG. 2. Monthly, zonal-mean daytime LWP values (mg cm^{-2}) derived from ISCCP (solid curves) and SSM/I (broken curves) for warm nonprecipitating clouds for August 1987 (upper left), November 1987 (upper right), February 1988 (lower left), and May 1988 (lower right). Note that Figs. 3 and 4 have the same order.

track regions. These LWP values are smaller than for warm clouds, except in the midlatitudes. In the Tropics, cold anvil clouds gain much of their water supply from their related convective systems (Gamache 1990). Surface and aircraft observations find that the glaciation temperature for convective systems is usually higher than −10°C (Gamache 1990; Hobbs and Rangno 1985), which is generally warmer than that for stratiform clouds in the midlatitudes, and that the base of the stratiform anvils is near the freezing level, so that ice is the dominant water component (Gamache 1990). The Southern Hemisphere midlatitudes exhibit small seasonal variation: the peak LWP in cold clouds is about 30%–50% larger than in warm clouds (cf. Fig. 2 and 3). The Northern Hemisphere midlatitudes exhibit a significant seasonal cycle, with LWP in cold clouds being largest in wintertime, but LWP in warm clouds is slightly larger in summertime. This variation seems consistent with the seasonal variations in the frequency and intensity of cyclone storms and with the generally stronger supercooling encountered in midlatitude clouds (Hobbs and Rangno 1985).

For cold nonprecipitating clouds, the ISCCP WP values are both much larger than the SSM/I LWP values and considerably more variable with latitude. The general features of the WP values for the 4 months follow the variations of the total cloud cover and cloud-top pressure patterns (Rossow et al. 1993), with a maximum in the Tropics (about 10–15 mg cm^{-2}), maxima in midlatitudes (about 15–20 mg cm^{-2}), and minima in the subtropics (around 7–10 mg cm^{-2}). The larger WP values for cold clouds are associated with regions of climatological atmospheric ascent, the upwelling part of the Hadley circulation in the Tropics, and eddy motions in the midlatitudes, while the subtropics are regions of average subsidence, and the cloud amounts

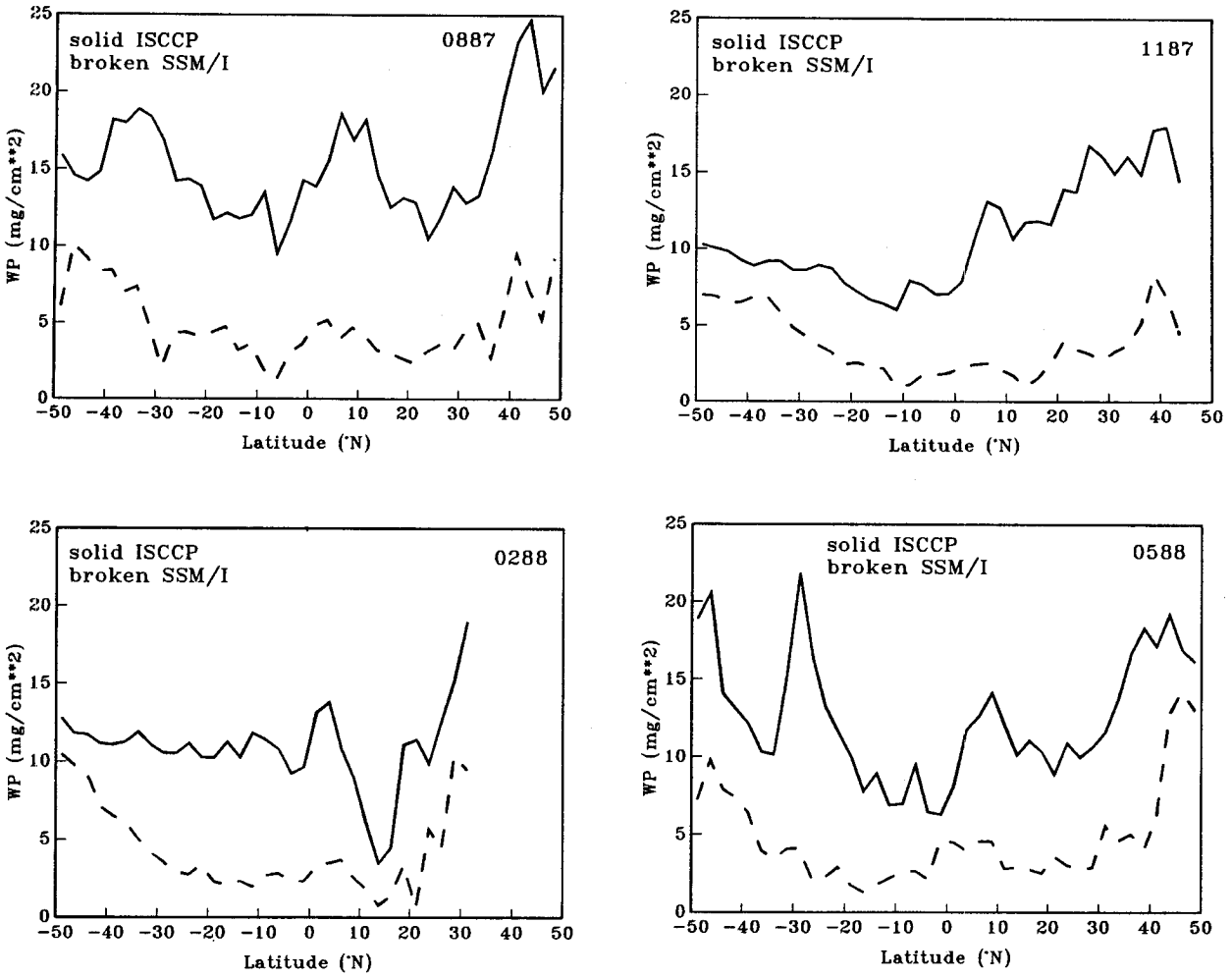

FIG. 3. Same as in Fig. 2 but for cold nonprecipitating clouds. Note that the ISCCP values represent total WP (in mg cm^{-2}).

and WP values are lower. The total water path seems to be largest in the summer midlatitudes.

We interpret the larger WP values from ISCCP in excess of the LWP from SSM/I as being caused by the presence of ice above the liquid parts of clouds or of ice cloud layers overlying liquid cloud layers. Since the visible radiances from which the ISCCP WP values are obtained are nearly as sensitive to ice as to water, whereas the SSM/I radiances are not sensitive to ice, the results in Fig. 3 are not surprising. Figure 4 exhibits the differences of the ISCCP WP and SSM/I LWP, which we take to be the ice water path for the 4 months, along with the average LWP for both warm and cold nonprecipitating clouds.

The general tendency of the latitude variations of IWP reflects the variations in high-level cloud amount, with minima in the subtropics and maxima in the Tropics and the midlatitudes. The latitude variations of the LWP averaged over both warm and cold nonprecipitating clouds are generally weaker than for IWP. Overall, IWP (about 7 mg cm^{-2}, but ranging from 3 to 17 mg cm^{-2}) is about 50% larger than warm and cold LWP (about 5 mg cm^{-2}). The equinoctial seasons show a significant gradient of IWP from a maximum of about 13 mg cm^{-2} in the autumn hemisphere to a minimum of about 3–5 mg cm^{-2} in the spring hemisphere. The winter and summer distributions are more uniform with latitude, but the August 1987 values of IWP are considerably larger than the February 1988 values. The larger values of IWP in August 1987 may not be normal for this season, since this particular month is at the end of an ENSO event. More data from other years must be analyzed to improve the description of seasonal changes.

Because of the change of cloud water phase with temperature, the colder hemispheres usually have more IWP than LWP than the warmer hemispheres. Again, August 1987 is an exception; in this month, the warm Northern Hemisphere seemed to hold more cloud ice water than its cold counterpart, but nevertheless, the

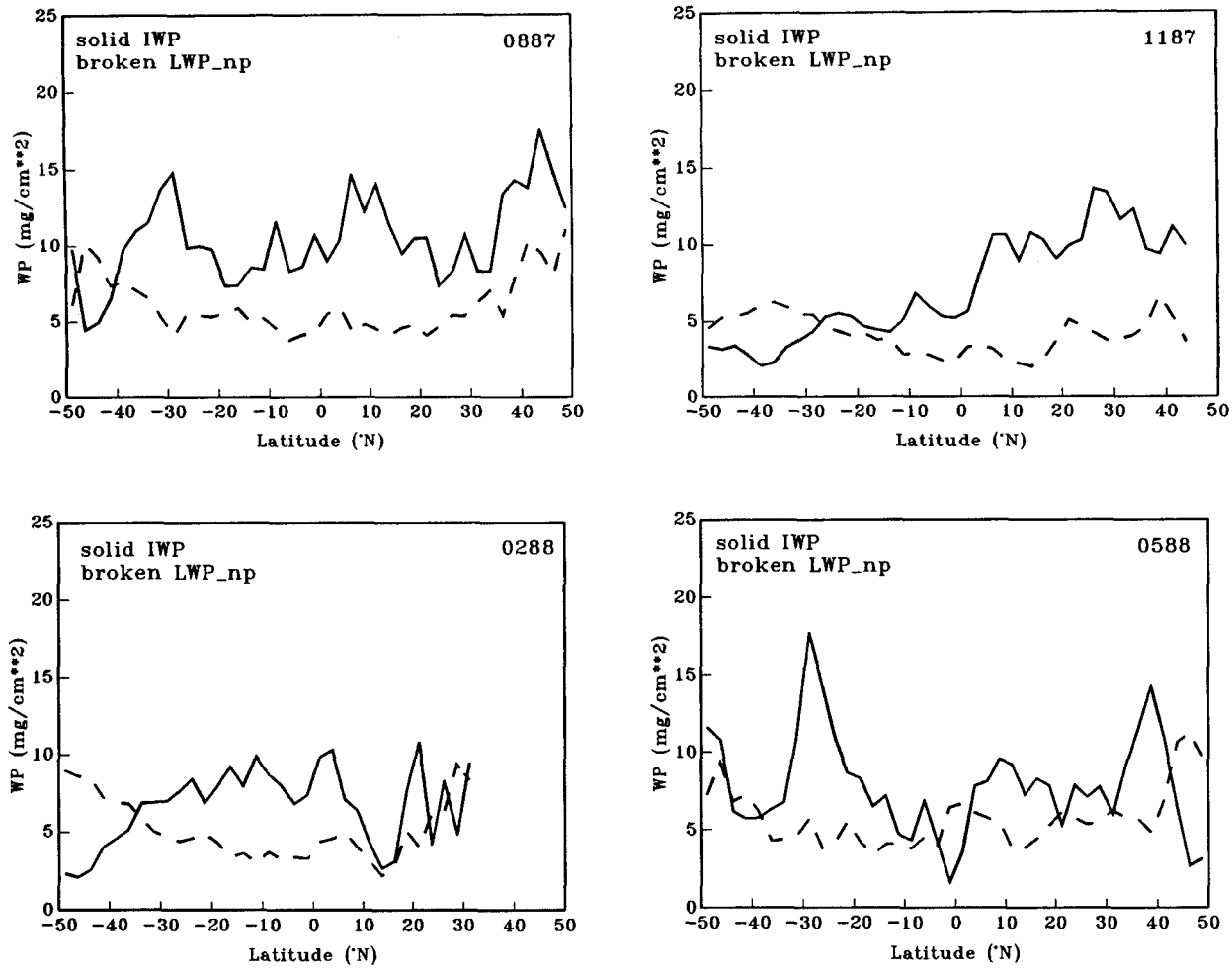

FIG. 4. Same as in Fig. 2 but for cloud ice water path (in mg cm^{-2}; solid lines), calculated as the difference between ISCCP WP and SSM/I LWP for cold nonprecipitating clouds and the average SSM/I LWP values for both warm and cold nonprecipitating clouds (in mg cm^{-2}; broken lines).

IWPs for the two hemispheres were similar. The seasonal change in the annual cycle of our study may be dominated more by changes in the number of precipitating systems than by the amount of water in each system (cf. Lin 1995; Chiu et al. 1993).

In Figure 5 we estimate a water-to-ice transition temperature, the temperature at which there is an equal probability of ice water and liquid water, from the distribution of average ice fraction with cloud-top temperature T_c. Ice fraction is defined as the ratio of IWP to total WP. Different curves for each month illustrate the seasonal variation for different climate regimes. Generally, ice fraction increases with decreasing T_c, as expected, with global values reaching 50% at about −15°C. Because ice cloud layers can overlie liquid water cloud layers (cf. Warren et al. 1985), the ice fraction need never reach 100%; indeed, the maximum fractions are only about 80% globally, and the fraction even decreases slightly for very cold T_c, where thin cirrus dominate. Likewise, since the ISCCP analysis for an optically thin ice cloud over a low-level liquid water cloud may overestimate the cloud-top temperature of the uppermost cloud layer (cf. Minnis et al. 1993b; Liao et al. 1995), the ice fraction will not go to zero at 0°C. The overall transition temperature of −15°C is in the range of other observations (cf. Feigelson 1984; Hobbs and Rangno 1985), but there are notable variations among climate regimes and with season.

Clouds in the Tropics show a transition temperature, about −8°C, that is warmer than the global average and does not vary much with season. Overall, the ice fractions for tropical clouds are higher than in the midlatitudes. Clouds in the northern midlatitudes have transition temperatures (about −5°C) in autumn that are similar or slightly larger than in the Tropics, but they decrease by about 10°C in spring. Winter and summer midlatitudes exhibit intermediate values. Overall ice fractions in the northern midlatitudes are smaller than

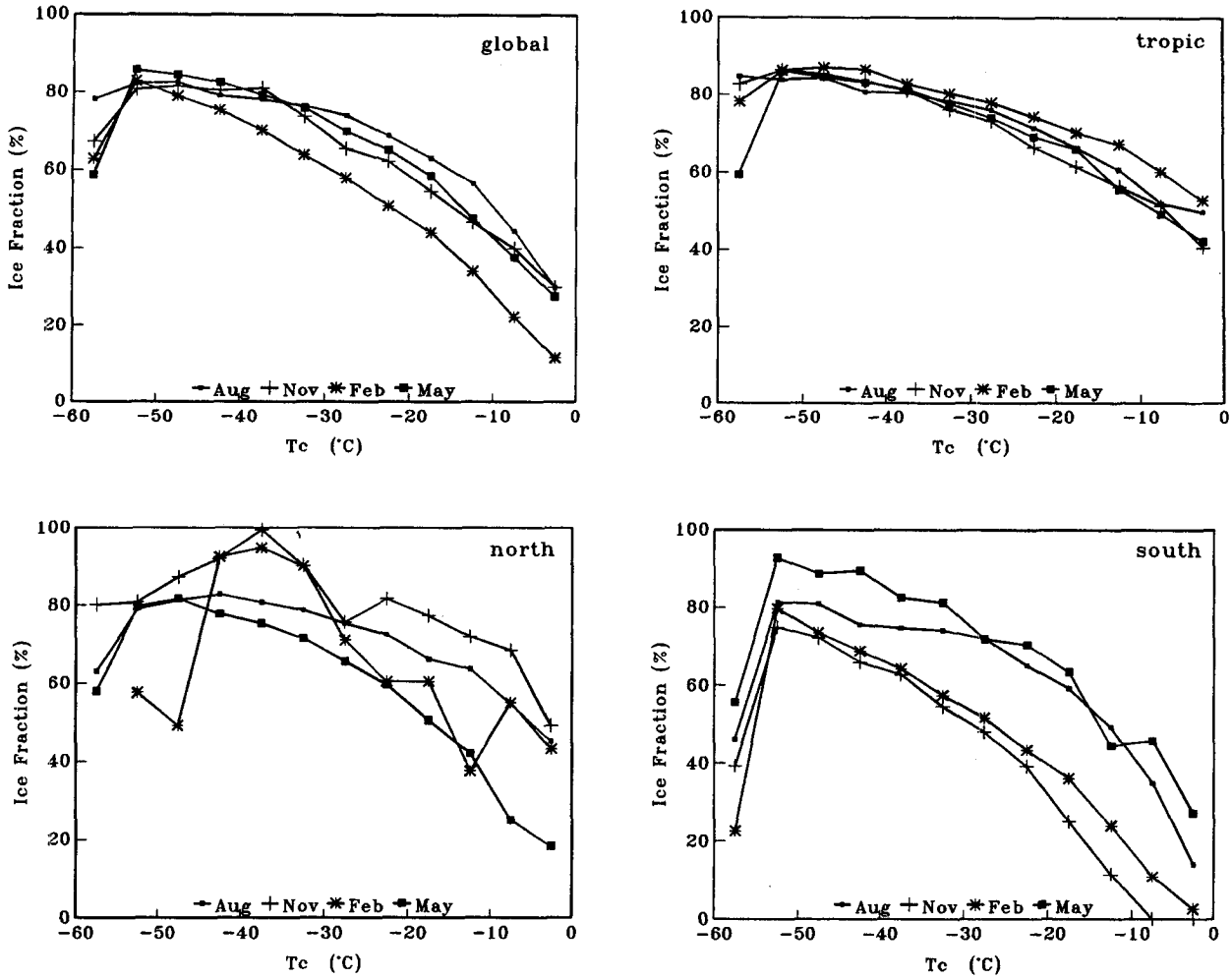

FIG. 5. Variation of cloud ice fraction (IWP/WP) with cloud-top temperature for global (upper left), tropical (upper right), northern midlatitudes (lower left), and southern midlatitudes (lower right) regimes. The curves with small squares, crosses, stars, and big squares represent the results for August 1987, November 1987, February 1988, and May 1988, respectively.

in the Tropics, but larger than in the southern midlatitudes. Clouds in the southern midlatitudes show the same seasonal amplitude and phase (with a hint of some lag) in the transition temperatures as in the north, but they are about 10°C colder on average.

Figures 3 and 4 show that the global ratio of IWP to LWP for cold nonprecipitating clouds over oceans is generally greater than 1, about 1.5 (Table 2). Combining both cold and warm nonprecipitating clouds gives a ratio of about 0.7 (since there is no IWP in warm clouds; Table 2), consistent with the simple theoretical estimate made in the appendix. However, Figs. 2 and 3 show that there is more latitude and seasonal variation in the IWP and LWP in cold clouds than in warm clouds. Thus, IWP/LWP in cold clouds varies from about 0.6 in the southern midlatitudes in the spring to almost 3 in the northern midlatitudes in the fall (cf. Table 2).

4. Discussion

We have used 4 months of SSM/I and ISCCP data to provide a first estimate of the seasonal variations of LWP and IWP in nonprecipitating clouds. The average LWP in warm-topped, nonprecipitating clouds is about 6 mg cm^{-2} and exhibits little variation with latitude or season. The average LWP in cold-topped, nonprecipitating clouds is about 4 mg cm^{-2}, varying from about 2–3 mg cm^{-2} in the Tropics to about 10 mg cm^{-2} in midlatitude storm track regions, with a weak seasonal variation at higher latitudes. The IWP in cold-topped, nonprecipitating clouds exhibits much more variation with latitude and season. Fall–winter midlatitudes usually have higher values (around 8–12 mg cm^{-2}) than the spring–summer midlatitudes (about 5–10 mg cm^{-2}). Tropical values of IWP are about 5–10 mg cm^{-2}. Overall, IWP is about 7 mg cm^{-2}, about

TABLE 2. Average ratio of IWP to LWP for cold nonprecipitating clouds (CNP), warm nonprecipitating clouds (WNP), and all nonprecipitating clouds (NP) for the global, Tropics, northern midlatitudes, and southern midlatitudes regimes. Annual mean is the average of the 4 months.

		August 1987	November 1987	February 1988	May 1988	Annual
Globe	CNP	2.28	1.07	1.17	2.00	1.42
	WNP	0.0	0.0	0.0	0.0	0.0
	NP	0.91	0.62	0.57	1.02	0.71
Tropics	CNP	3.37	4.05	4.26	2.59	3.61
	WNP	0.0	0.0	0.0	0.0	0.0
	NP	1.24	2.04	2.07	1.29	1.55
Northern midlatitudes	CNP	2.66	2.64	1.32	1.36	1.95
	WNP	0.0	0.0	0.0	0.0	0.0
	NP	0.87	1.28	0.42	0.70	0.84
Southern midlatitudes	CNP	1.49	0.56	0.71	2.79	0.81
	WNP	0.0	0.0	0.0	0.0	0.0
	NP	0.76	0.36	0.35	1.52	0.44

50% larger than LWP *in cold-topped,* nonprecipitating clouds; but this ratio ranges from about 3 in the northern midlatitudes in summer–fall and in the Tropics to about 0.6 at higher latitudes in the Southern Hemisphere in spring–summer (cf. Table 2). Combining the IWP and LWP values from both warm and cold nonprecipitating clouds gives a ratio, IWP/LWP, of about 0.7 (Table 2).

The uncertainty in these IWP estimates is large, the primary sources being errors in SSM/I LWP retrievals, errors in the ISCCP optical thickness retrievals, and errors in Eq. (1) used to convert optical thicknesses to WP. In addition, the effects of mismatched fields of view and the possible presence of multilayered clouds (and some associated errors in the ISCCP cloud-top temperatures) can confuse the interpretation of the results.

The matching of ISCCP and SSM/I pixels is exploited in several ways in our analysis, but the most important purpose is to select cloud-free SSM/I pixels for fine-tuning the LWP retrieval to remove biases associated with errors in both surface properties and the absorption properties of liquid water and water vapor. Once tuned, the SSM/I data could be used alone to obtain average LWP values in nonprecipitating clouds, but there would be biases caused by neglecting the variations of liquid water temperature and by attempting to separate clear and cloudy scenes (Lin and Rossow 1994). Likewise, the total WP could be determined from ISCCP alone, although there would be a bias from including precipitating clouds. Hence, the average difference between WP and LWP, interpreted in terms of IWP, could have been obtained from a separate analysis of the two datasets, followed by taking the difference, without the matching procedure (except for the SSM/I retrieval tuning). Although the time and location differences that we allow can mean that individual clouds are not well represented by the ISCCP and SSM/I pixels, there is a beneficial reduction of retrieval biases obtained by accounting for systematic temperature variations and eliminating clear scenes and precipitating clouds. The actual pixels should be thought of as samples of the area-averaged cloud properties; biases will arise only if these samples are biased (see discussion in Seze and Rossow 1991; Rossow et al. 1993). Since the majority of observations are used in this approach, we argue that the *average* values of WP and LWP are not much affected by the statistical effects of pixel mismatches unless they systematically alter detections of clear conditions, precipitating clouds, or cloud-top temperatures.

The occurrence of multilayer clouds means that we cannot distinguish in our results among deep cloud layers composed of a liquid lower part and an ice upper part, cloud layers that might be a mixture of phases, and separate cloud layers with different phases. Nevertheless, all these cases contribute to the total IWP and LWP, so there is no bias associated with averaging these different cases together.

The last situation also leads to errors in the retrieved cloud-top temperatures in the ISCCP results, but only if the upper cloud layer is optically thin. Note that estimated errors in ISCCP cloud-top temperatures for low-level clouds are <3°C (e.g., Wang and Rossow 1995; cf. Minnis et al. 1992). An independent comparison of ISCCP cloud-top locations for high-level clouds with the Stratospheric Aerosol and Gas Experiment II limb scanning results (Liao et al. 1995) does indicate a bias equivalent to cloud-top temperatures that are too large by 3°–6°. The magnitude of this effect is largest for the lowest optical thicknesses of the upper layer; hence, the misclassification of a cloud as a warm cloud when there is some ice in the column becomes most significant as the amount of ice goes to zero, which does not cause much error in IWP. In fact, our cloud-top temperature threshold for separating all liquid from mixed-phase clouds is set at 0°C, which is 5° to 10° warmer than the expected transition freezing temperature, for this reason. However, a tendency to underestimate IWP at higher temperatures suggests that

our transition temperatures may be lower than the actual average freezing temperature. In addition, the occurrence of cirrus over liquid boundary layer clouds also lowers the average transition temperature.

The possible sources of error in the SSM/I retrievals of LWP and their magnitudes are thoroughly discussed in Lin and Rossow (1994). The most significant bias in an analysis of SSM/I only is that it cannot separate clear from cloudy conditions, so that average LWP values may be biased low by including clear regions in the average (Lin and Rossow 1994). The dependence of the liquid water microwave absorption on temperature is accounted for in our analysis by using the ISCCP cloud-top temperatures, which causes a small underestimate of LWP compared with using the larger absorption-weighted average of water temperature over the whole cloud layer. This effect is partially offset, however, by some tendency for the ISCCP cloud-top temperatures to be a few degrees too large. In cold clouds, the lowest water temperature is taken to be 0°C, which would lead to an overestimate of LWP if most of the liquid water is supercooled. In any case, the magnitude of these effects is no more than 2 mg cm^{-2} if the temperature errors are no more than 6°C (Lin and Rossow 1994). We emphasize here that the sensitivity of the SSM/I to liquid water, together with uncertainties in the absorption coefficients and surface properties, makes the accuracy of *individual* SSM/I retrievals low, but that use of other information to specify surface properties and cloud temperature and to identify clouds significantly reduces possible biases (Lin and Rossow 1994).

Thus, we consider the major uncertainties in the IWP values to arise from the ISCCP retrievals of cloud optical thicknesses when ice particles are present and from specifying the size and shape of the particles. The latter is the largest single source of uncertainty.

The ISCCP analysis relates the visible optical thicknesses to visible radiances using a radiative transfer model that assumes the cloud to be composed of spherical liquid water droplets specified by a gamma distribution with an effective particle radius, $r_e = 10$ μm, and an effective size variance of 0.15. A recent survey of effective droplet radii in liquid water clouds showed that the global-mean value of r_e is about 11.5 μm, about 12 μm over oceans and about 8.5 μm over land (Han et al. 1994), implying *average* errors in the ISCCP optical thicknesses for warm clouds that are <3% and that are <20% in LWP for warm clouds.

To obtain a more accurate estimate of WP for ice clouds, Eq. (1) needs to be changed in three ways. First, the retrieved values of cloud optical thickness τ need to be corrected by using a scattering phase function that is more representative of ice crystal size and shape effects (Wielicki et al. 1990; Baum et al. 1992; Minnis et al. 1993a,b). When this is done, the estimated change in τ is a decrease by about a factor of 2 on average (Minnis et al. 1993b; Mishchenko et al. 1996). Note, however, that if a cloud is composed of both ice and liquid, then the retrieved optical thickness will be intermediate between the pure ice and pure liquid values (Sun and Shine 1994), reducing the needed correction factor.

Second, the effective value of r_e must be increased (e.g., Heymsfield 1977; Hobbs and Rangno 1985; Heymsfield and Donner 1990), but the nonspherical shape and the frequent occurrence of very broad size distributions in ice clouds (e.g., Burkovskaya et al. 1991; Francis 1995) complicate an estimate of a proper value. Various authors have suggested effective sizes ranging from 30 to 100 μm (e.g., Wielicki et al. 1990; Francis 1995), but we lack comprehensive global surveys of ice crystal sizes and shapes. Preliminary results of a global survey of ice crystal sizes using Advanced Very High Resolution Radiometer measurements (Q. Han, 1995, personal communication) suggest a global-mean value of 28 μm with systematic regional variations of about 50%. However, this "optical" value applies at cloud tops. Since larger crystals are often found near cloud base, the overall average size may be larger. In any case, the estimated change in r_e is an increase by at least a factor of 3 on average.

Third, the precise value of the numerical coefficient in Eq. (1) depends on the particle density and the geometric relationship of the particle cross section and volume, as well as the scattering efficiency, which also depends on wavelength. The main uncertainty is what "effective" particle density to assume—that is, the ratio of actual particle volume to the volume of a sphere with the same scattering cross section times the bulk density. The bulk density of pure ice is about 0.92 g cm^{-3}, but the density of amorphous ice with air bubbles can be as small as 0.7 g cm^{-3} (Hobbs 1974). Observations of large (dimensions > 100 μm) composite particles suggest effective densities as low as 0.1 (e.g., Locatelli and Hobbs 1974); however, smaller (dimensions < 100 μm) particles appear more to be compact (cf. Francis 1995) with higher effective densities. Heymsfield (1972) proposes effective densities for bullets and columns of about 0.45 and 0.65, respectively. For the fractal particle studied by Mishchenko et al. (1996), the effective density is 0.62. Thus, the coefficient in Eq. (1) should be reduced by at least a factor of 2.

In summary, the first and third factors reduce the estimated IWP by about a factor of 4, whereas the second factor increases it by at least a factor of 3. Thus, the values for IWP obtained here may be underestimates. We note that in the new ISCCP retrieval procedure, which treats cold clouds (cloud-top temperatures < 260 K) as pure ice with 30-μm fractal crystals (Mishchenko et al. 1996), the WP values obtained from Eq. (1) with the "correct" factors are almost unchanged from the values obtained here using the parameter values for a liquid water cloud. Because there are significant regional variations of the average par-

ticle size (the most important error source), the uncertainties in IWP must still be assumed to be as much as 50% to 100%, but are unlikely to be as large as an order of magnitude. If a size estimate of 30 μm is too low, the Eq. (1) underestimates IWP and IWP/LWP could be >1 (see appendix).

Acknowledgments. We would like to express our appreciation to Tony Del Genio, David Rind, and Bruce Wielicki for their helpful comments. We also thank two anonymous reviewers for extensive comments that helped focus the discussion. The National Aeronautics and Space Administration (NASA) WetNet project provided SSM/I data and technical assistance. This study is supported by the NASA Global Radiation Data Analysis and Modeling Program. One of our authors (BL) also acknowledges support from NASA Clouds and the Earth's Radiant Energy System under Contract NAS1-19656.

APPENDIX

Theoretical Estimates of IWP/LWP

A simple theoretical estimate of the average value of IWP/LWP can be obtained by calculating the amount of water condensed from saturated parcels lifted over 10-mb intervals at each level in the U.S. Standard Atmosphere (surface temperature = 15°C) between a lifting condensation level at 0.9 km (temperature = 9.2°C) and the tropopause at 11 km (temperature = −55°C). A lifting condensation level occurs at 0.9 km for an average surface relative humidity of 75% and is consistent with available observations (e.g., Wang and Rossow 1995). Different absolute amounts of water would be condensed for different lifting intervals, but the ratios of column water amounts remain approximately the same. This calculation is equivalent to assuming that the vertical distribution of condensed water is at least proportional to the vertical distribution of saturation vapor pressure. For a freezing temperature of −4°C over oceans (Hobbs and Rangno 1985), IWP/LWP ≈ 0.9; for a range of freezing temperatures from 0° to −15°C, the ratio varies from 1.6 to 0.3. The actual global average of this ratio will be altered by the nonuniform distribution of clouds with altitude, latitude, and season. The ISCCP observations suggest that cloud optical thicknesses (proportional to WP) are generally larger for higher cloud tops (Rossow and Schiffer 1991) and larger at higher latitudes and in colder seasons (Tselioudis et al. 1992). Both of these facts suggest that the actual distribution of clouds may increase the value of IWP/LWP compared with this calculation.

REFERENCES

Adler, R. F., R. A. Mack, N. Prasad, H.-Y. M. Yeh, and I. M. Hakkarinen, 1990: Aircraft microwave observations and simulations of deep convection from 18 to 183 GHz. Part I: Observations. *J. Atmos. Oceanic Technol.*, **7,** 377–391.

——, H.-Y. Yeh, N. Prasad, W.-K. Tao, and J. Simpson, 1991: Microwave simulations of a tropical rainfall system with a three-dimensional cloud model. *J. Appl. Meteor.*, **30,** 924–953.

Baum, B. A., B. A. Wielicki, P. Minnis, and L. Parker, 1992: Cloud-property retrieval using merged HIRS and AVHHR data. *J. Appl. Meteor.*, **31,** 351–369.

Blaskovic, M., R. Davies, and J. B. Snider, 1991: Diurnal variation of marine stratocumulus over San Nicolas Island during July 1987. *Mon. Wea. Rev.*, **119,** 1469–1478.

Burkovskaya, S. N., A. L. Kosarev, and A. Y. Naumov, 1991: Investigation of cirrus microstructure on May 15, 1989. *Izv. Akad. Nauk SSR, Atmos. Oceanic Phys.*, **27,** 714–724.

Carlson, B., A. A. Lacis, and W. B. Rossow, 1993: Tropospheric gas composition and cloud structure of the Jovian north equatorial belt. *J. Geophys. Res.*, **98,** 5251–5290.

Chiu, L. S., A. T. C. Chang, and J. Janowiak, 1993: Comparison of monthly rain rates derived from GPI and SSM/I using probability distribution functions. *J. Appl. Meteor.*, **32,** 323–334.

Del Genio, A. D., 1993: Convective and large-scale cloud processes in global climate models. *Proceedings of Energy and Water Cycle in the Climate System,* E. Rasche and D. Jacob, Eds., NATO Advanced Study Institute, 95–121.

——, M.-S. Yao, W. Kovari, and K. K.-W. Lo, 1996: A prognostic cloud water parameterization for global climate models. *J. Climate,* **9,** 270–304.

Fairall, C. W., J. E. Hare, and J. B. Snider, 1990: An eight-month sample of marine stratocumulus cloud fraction, albedo, and integrated liquid water. *J. Climate,* **3,** 847–864.

Feigelson, E. M., 1984: *Radiation in a Cloudy Atmosphere.* D. Reidel, 293 pp.

Francis, P. N., 1995: Some aircraft observations of the scattering properties of ice crystals. *J. Atmos. Sci.*, **52,** 1142–1154.

Gamache, J. F., 1990: Microphysical observations in summer MONEX convective and stratiform clouds. *Mon. Wea. Rev.*, **118,** 1238–1249.

Goodberlet, M. A., C. T. Swift, and J. C. Wilkerson, 1990: Ocean surface wind speed measurements of Spacial Sensor Microwave/Imager (SSM/I). *IEEE Trans. Geosci. Electron.*, **GE-28,** 832–828.

Greenwald, T. J., G. L. Stephens, T. H. Vonder Haar, and D. L. Jackson, 1993: A physical retrieval of cloud liquid water over the global oceans using SSM/I observations. *J. Geophys. Res.*, **98,** 18 471–18 488.

Han, Q., W. B. Rossow, and A. A. Lacis, 1994: Nearly global survey of effective droplet radii in liquid water clouds using ISCCP data. *J. Climate,* **7,** 465–497.

Heymsfield, A. J., 1972: Ice crystal terminal velocities. *J. Atmos. Sci.*, **29,** 1348–1357.

——, 1977: Precipitation development in stratiform ice clouds: A microphysical and dynamical study. *J. Atmos. Sci.*, **34,** 367–381.

——, and L. J. Donner, 1990: A scheme for parameterizing ice cloud water content in general circulation models. *J. Atmos. Sci.*, **47,** 1865–1877.

Hobbs, P. V., 1974: *Ice Physics.* Clarendon, 662–667.

——, and A. L. Rangno, 1985: Ice particle concentrations in clouds. *J. Atmos. Sci.*, **42,** 2523–2549.

Li, Z., and H. Le Treut, 1992: Cloud radiation feedbacks in a general circulation model and their dependence on cloud modelling assumptions. *Climate Dyn.*, **7,** 133–139.

Liao, X., W. B. Rossow, and D. Rind, 1995: Comparison between SAGE II and ISCCP high-level clouds. Part II: Locating cloud-tops. *J. Geophys. Res.*, **100,** 1137–1147.

Lin, B., 1995: Observations of cloud water path and precipitation over oceans using ISCCP and SSM/I data. Ph.D. dissertation, Columbia University, 315 pp.

——, and W. B. Rossow, 1994: Observations of cloud liquid water path over oceans: Optical and microwave remote sensing methods. *J. Geophys. Res.*, **99,** 20 907–20 927.

Liu, G., and J. A. Curry, 1992: Retrieval of precipitation from satellite microwave measurements using both emission and scattering. *J. Geophys. Res.*, **97,** 9959–9974.

——, and ——, 1993: Determination of characteristic features of cloud liquid water from satellite microwave measurements. *J. Geophys. Res.*, **98,** 5069–5092.

Locatelli, J. D., and P. V. Hobbs, 1974: Fall speeds and masses of solid precipitation particles. *J. Geophys. Res.*, **79,** 2185–2197.

Minnis, P., P. W. Heck, D. F. Young, C. W. Fairall, and J. B. Snider, 1992: Stratocumulus cloud properties derived from simultaneous satellite and island-based instrumentation during FIRE. *J. Appl. Meteor.*, **31,** 317–339.

——, K. N. Liou, and Y. Takano, 1993a: Inference of cirrus cloud properties using satellite-observed visible and infrared radiances. Part I: Parameterization of radiance fields. *J. Atmos. Sci.*, **50,** 1279–1304.

——, P. W. Heck, and D. F. Young, 1993b: Inference of cirrus cloud properties using satellite-observed visible and infrared radiances. Part II: Verification of theoretical cirrus radiative properties. *J. Atmos. Sci.*, **50,** 1305–1322.

Mishchenko, M. I., W. B. Rossow, A. Macke, and A. A. Lacis, 1996: Sensitivity of cirrus cloud albedo, bidirectional reflectance, and optical thickness retrieval accuracy to ice-particle shape. *J. Geophys. Res.*, **101,** 16 973–16 985.

Mitchell, J. F. B., C. A. Senior, and W. J. Ingram, 1989: CO_2 and climate: A missing feedback? *Nature,* **341,** 132–134.

Mugnai, A., and E. A. Smith, 1988: Radiative transfer to space through a precipitating cloud at multiple microwave frequencies. Part I: Model description. *J. Appl. Meteor.*, **27,** 1055–1073.

Peixoto, J. P., and A. H. Oort, 1992: *Physics of Climate.* Amer. Inst. Phys., 520 pp.

Petty, G. W., 1990: On the response of the special sensor microwave/imager to the marine environment: Implications for atmospheric parameter retrievals. Ph.D. dissertation, University of Washington, 292 pp.

Platt, C. M. R., J. C. Scott, and A. C. Dilley, 1987: Remote sounding of high clouds. Part VI: Optical properties of midlatitude and tropical cirrus. *J. Atmos. Sci.*, **44,** 729–747.

Ropelewski, C. F., 1988: The global climate for June–August 1988: A swing to the positive phase of the Southern Oscillation, drought in the United States, and abundant rain in monsoon areas. *J. Climate,* **1,** 1153–1174.

Rossow, W. B., and A. A. Lacis, 1990: Global, seasonal cloud variations from satellite radiance measurements. Part II: Cloud properties and radiative effects. *J. Climate,* **3,** 1204–1253.

——, and R. A. Schiffer, 1991: ISCCP cloud data products. *Bull. Amer. Meteor. Soc.*, **72,** 2–20.

——, and L. C. Garder, 1993: Cloud detection using measurements of infrared and visible radiances for ISCCP. *J. Climate,* **6,** 2341–2369.

——, and Y.-C. Zhang, 1995: Calculation of surface and top-of-atmosphere radiative fluxes from physical quantities based on ISCCP datasets. Part II: Validation and first results. *J. Geophys. Res.*, **100,** 1167–1197.

——, L. C. Garder, and A. A. Lacis, 1989: Global, seasonal cloud variations from satellite radiance measurements. Part I: Sensitivity of analysis. *J. Climate,* **2,** 419–462.

——, ——, P.-J. Lu, and A. Walker, 1991: International Satellite Cloud Climatology Project (ISCCP) documentation of cloud data. WMO/TD 266, World Climate Research Programme (ICSU and WMO), Geneva, Switzerland, 76 pp.

——, A. W. Walker, and L. C. Garder, 1993: Comparison of ISCCP and other cloud amounts. *J. Climate,* **6,** 2394–2418.

Sassen, K., 1991: The polarization lidar technique for cloud research: A review and current assessment. *Bull. Amer. Meteor. Soc.*, **72,** 1848–1866.

——, and H. Zhao, 1993: Supercooled liquid water clouds in Utah winter mountain storms: Cloud-seeding implications of a remote sensing dataset. *J. Appl. Meteor.*, **32,** 1548–1558.

——, D. Starr, and T. Uttal, 1989: Mesoscale and microscale structure of cirrus clouds: Three case studies. *J. Atmos. Sci.*, **46,** 371–396.

Seze, G., and W. B. Rossow, 1991: Effects of satellite data resolution on measuring the space/time variations of surfaces and clouds. *Int. J. Remote Sensing,* **12,** 921–952.

Sheu, R.-S., and G. Liu, 1995: Atmospheric humidity variations associated with westerly wind bursts during TOGA COARE. *J. Geophys. Res.*, **100,** 25 759–25 768.

Smith, E. A., and A. Mugnai, 1988: Radiative transfer to space through a precipitating cloud at multiple microwave frequencies. Part II: Results and analysis. *J. Appl. Meteor.*, **27,** 1074–1091.

Smith, R. N. B., 1990: A scheme for predicting layer clouds and their water content in a general circulation model. *Quart. J. Roy. Meteor. Soc.*, **116,** 435–460.

Sun, Z., and K. P. Shine, 1994: Studies of the radiative properties of ice and mixed phase clouds. *Quart. J. Roy. Meteor. Soc.*, **120,** 111–137.

Tjemkes, S. A., G. L. Stephens, and D. L. Jackson, 1991: Spaceborne observation of column water vapor: SSMI observations and algorithm. *J. Geophys. Res.*, **96,** 10 941–10 954.

Tselioudis, G., W. Rossow, and D. Rind, 1992: Global patterns of cloud optical thickness variation with temperature. *J. Climate,* **5,** 1484–1495.

Wang, J., and W. B. Rossow, 1995: Determination of cloud vertical structure from upper-air observations. *J. Appl. Meteor.*, **34,** 2243–2258.

Warren, S. G., 1984: Optical constants of ice from the ultraviolet to the microwave. *Appl. Optics,* **23,** 1206–1255.

——, C. J. Hahn, and J. London, 1985: Simultaneous occurrence of different cloud types. *J. Climate Appl. Meteor.*, **24,** 658–667.

Wielicki, B. A., J. T. Suttles, A. J. Heymsfield, R. M. Welch, J. D. Spinhirne, M.-L. C. Wu, D. O. Starr, L. Parker, and R. F. Arduini, 1990: The 27–28 October 1986 FIRE IFO cirrus case study: Comparison of radiative transfer theory with observations by satellite and aircraft. *Mon. Wea. Rev.*, **118,** 2356–2376.

Wilheit, T. T., A. T. C. Chang, M. S. V. Rao, E. B. Rodgers, and J. S. Theon, 1977: A satellite technique for quantitatively mapping rainfall rates over the oceans. *J. Appl. Meteor.*, **16,** 551–560.

——, ——, and L. S. Chiu, 1991: Retrieval of monthly rainfall indices from microwave radiometric measurements using probability distribution functions. *J. Atmos. Oceanic Technol.*, **8,** 118–136.